Clustering of Hydrogen Molecules around a Molecular Cation: The $Li_3^+(H_2)_n$ Clusters ($n = 1 - 6$)

Mario Barbatti,[†] Ginette Jalbert,[‡] and Marco Antonio Chaer Nascimento*,[†]

Instituto de Quimica, Universidade Federal do Rio de Janeiro, Rio de Janeiro, 21949-900, RJ, Brazil, and Instituto de Fisica, Universidade Federal do Rio de Janeiro, CP 68528, Rio de Janeiro, 21945-970, RJ, Brazil

Ab initio calculations for the lowest-energy isomers of the clusters $Li_3^+(H_2)_n$ ($n = 0-6$) show that the first shell of H_2molecules is formed by attaching from one to four molecules independently to each vertex of the triangular Li_3^+ core. For $2 \leq n \leq 6$, several isomers are possible, depending on how the n ligands are distributed among the three vertexes. The binding energies are very similar to those obtained for the $Li^+(H_2)_n$ clusters, and they vary from 3 to 1.5 kcal/mol, depending on the size of the cluster. The reaction of formation of the cluster is more exothermic at temperatures between 150 and 200 K.

1. Introduction

In a series of papers,[1,2,3] we have investigated theoretically the structural properties of ionic hydrogen clusters formed by the clustering of the H_2 molecules around a coulombian field produced by simple atomic or molecular ions such as Li^+, Na^+, K^+, and H_3^+. These clusters, depending on the number of H_2 molecules attached to it, have binding energies between 0.5 and 5 kcal/mol and are produced in exothermic multiple-step reactions of the type

$$X^+ + (n+1)H_2 \rightarrow X^+(H_2)_n + H_2 \qquad (1)$$

In general, the structure of the cluster consists of a well-defined positive core around which the H_2 molecules are distributed. The core dominates the reactions of the cluster with other species. As an example, the electron capture in collisions with He atoms does not depend on the size of the cluster, but just on the core−He interaction.[4]

The H_2 molecules are distributed in shells around the core. In each shell, the number of H_2 molecules is such that the H_2-H_2 distance within the shell resembles that of the first-neighbors in solid hydrogen (3.8 Å). This is remarkable, since the van der Waals energy minimum for the H_2-H_2 energy is about 4.53 Å. The radius of the first shell, in the case of a triangular H_3^+ core, allows up to three H_2 molecules to be attached to it. For the case of the Li^+, this number increases to six.

The clustering of hydrogen molecules around a coulombian center has been studied theoretical and experimentally for a wide variety of cations such as the H_3^+ molecular ion,[1,3−8] the first-column Li^+, LiH^+, Na^+, and K^+[2,9], the second-column Be^+[10] and Mg^+[11], the Al^+ ion,[10,12] and the metals from Sc^+ to Zn^+[13,14] and, for the more complex molecular cores, CH_5^+,[15,16] $CH_3N_2^+$,[17] and N_2H^+.[18]

In the present work, we extend the research for the hydrogen clustering around the Li_3^+ cation. This cation has a triangular structure similar to that of the H_3^+ ion. Its electronic structure, however, resembles that of the Li^+ ion. The aim of this work is to compare the structures of the hydrogen clusters obtained from these three cores. As far as we are aware, these are the first results for the $Li_3^+(H_2)_n$ clusters.

* Corresponding author.
† Instituto de Quimica.
‡ Instituto de Fisica.

2. Method and Levels of Calculation

The method and the level of the calculation are similar to those from the ref 1−3. Briefly, self-consistent-field (SCF) Hartree−Fock (HF) calculations have been performed for the $Li_3^+(H_2)_n$ ($n = 0-6$) clusters using the 6-311G(d,p) and 6-311G-(2d,2p) polarized basis sets.[19] Electronic correlation effects have been taken into account by means of second and complete fourth-order Møller−Plesset perturbation theory (MP2 and MP4). The search for the equilibrium geometries was accomplished by means of an improved quasi-Newton−Raphson procedure and quadratic energy surface approximation. The criteria for geometry optimization were a maximum-energy gradient lower than 10^{-10} hartree/bohr and a root-mean-square energy gradient lower than $1/3 \times 10^{-10}$ hartree/bohr.

The geometries were optimized at the MP2/6-311G(d,p) level of theory, and for each optimized geometry, all the harmonic frequencies were verified to be real. At the MP2 optimized geometries, the energies were also computed at the complete MP4/6-311G(2d,2p). As we have discussed in ref 1, the MPn perturbative methods applied to the hydrogen clusters lead to satisfactory results when compared with the coupled cluster (CCSD(T)) results. The basis sets used also produce satisfactory Hartree−Fock energies when compared with larger basis such as the Dunning's cc-pVQZ basis set. All the ab initio calculations have been performed using the PC GAMESS version[20] of the GAMESS (US) QC package[21] and the Gaussian 94 package.[22] Basis set superposition errors were considered in all stages of the calculations.

3. Results and Discussion

3.1. Structure and Energy. The ground-state equilibrium structure of the Li_3^+ molecular ion is an equilateral triangle (D_{3h}), with sides equal to 3.011 Å. The linear geometry ($D_{\infty h}$) is not a minimum in the potential energy surface (PES), standing more than 17 kcal/mol (6273 cm^{-1}) above the ground state. This structure has two imaginary frequencies (105 cm^{-1}), each one corresponding to the transition between two minima through the 2-fold axis of symmetry perpendicular to the axis of the linear structure. The dissociation energies of the Li_3^+ ion and of the H_2 molecule, irrespective of the dissociation channel, are at least 1 order of magnitude higher than the binding energy of a typical monopole/induced-dipole bond in the hydrogen ionic

10.1021/jp013159m CCC: $22.00
Published on Web 12/20/2001

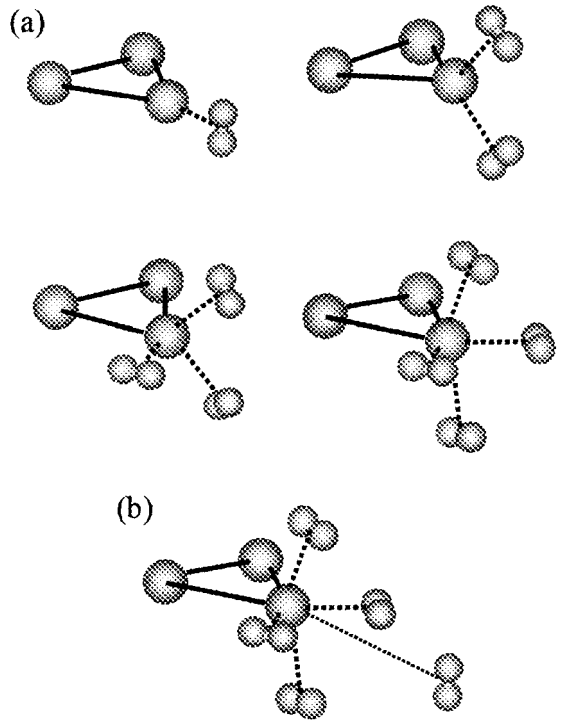

Figure 1. Structure of the $Li_3^+(H_2)_n$ clusters as predicted by the calculation at MP2/6-311G(d,p) level. (a) At each vertex of the Li_3^+ molecular ion, up to four H_2 molecules may be attached. (b) A fifth H_2 molecule attached at one vertex is in equilibrium at 3.92 Å from the vertex.

TABLE 1: Binding Energy for the Li_3^+, H_2, and $Li_3^+(H_2)$ Molecules Relative to the Main Dissociation Channels, Obtained at MP4/6-311G(2d,2p) Level, with BSSE Corrections

molecule	products	D_e (kcal/mol)
$Li_3^+(^1A_1')$	$Li_2^+(^2\Sigma_g) + Li(^2S)$	−34.7
	$Li_2(^1\Sigma_g) + Li^+(^1S)$	−42.2
	$Li^+(^1S) + 2Li(^2S)$	−64.0
$H_2(^1\Sigma_g^+)$	$2H(^2S)$	−107.3
$Li_3^+(H_2)(^1A_1)$	$Li_3^+(^1A_1') + H_2(^1\Sigma_g^+)$	−3.1

clusters (Table 1). Thus, once in the presence of an H_2 atmosphere, the Li_3^+ cation will prefer to behave as a coulombian core for hydrogen clustering other than to react with the H_2 molecules to produce lithium hydrides. In fact, independently of the initial configuration of the system, the optimization process always leads to structures with the H_2 molecules spherically distributed around the vertexes of the Li_3^+ core.

On each vertex V_k of the Li_3^+ core, one may attach up to four H_2 molecules (Figure 1a), all of them standing approximately 2.1 Å from the closest lithium atom, which is the same distance found in the $Li^+(H_2)_n$ clusters.[2] Any attempt to add a fifth H_2 unit to a vertex results in the migration of this extra unit to a more external position (outer shell) (Figure 1b) or to the neighborhood of another less occupied vertex. This establishes a pattern for building up these clusters: the first H_2 units will bind to the Li_3^+ core, a maximum of four units per Li atom, to form the first shell of ligands (see Figure 2). Of course, for a given number of H_2 units, there will be several ways of distributing these ligands in the first shell. When n exceeds the occupation number for the first shell, the additional molecules will start to occupy positions in the outer shell of ligands.

We studied all isomers formed from the different ways of distributing n H_2 molecules in the first shell, for $n = 0-6$, which is the limit of our present computational capabilities for the level of calculation employed. The geometrical parameters are given in Table 2. The absolute energies for the studied isomers and also their energies relative to the most stable isomer (ΔE), for each n, are shown in Table 3. The Mülliken charges are given in Table 4. It is important to have in mind that due to the small difference in energy among distinct isomers of a given cluster, the level of theory employed may not be accurate enough to distinguish them. To test the accuracy of the relative energies obtained at the MP4 level, we have calculated single-point energies for the isomers $i = 0$ and $i = 1$ for the $n = 5$ cluster, at the CCSD(T)/6-311G(2d,2p) level. The ΔE obtained at the

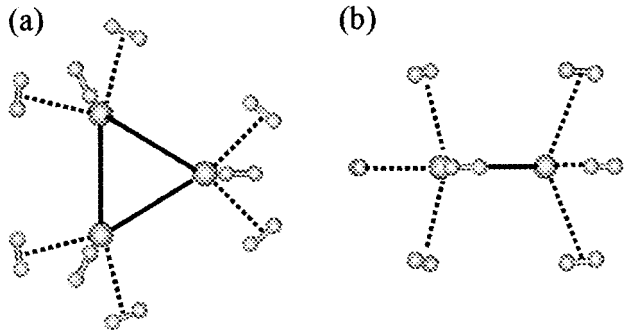

Figure 2. Possible structure of the $Li_3^+(H_2)_{12}$ cluster, as predicted by the calculation at MP2/6-311G(d,p) level. The molecular symmetry during the optimization procedure was restricted to the point group D_{3h} and the vibrational frequencies were not calculated. Views (a) perpendicular and (b) parallel to the Li_3^+ plane.

TABLE 2: Geometric Parameters as Predicted by the Calculations at MP2/6-311G(d,p) Level (in Å)[a]

	R (Å)	ρ (Å)	r (Å)	D (Å)
first shell	3.01 ± 0.08	2.12 ± 0.02	0.744 ± 0.001	2.98 ± 0.05
second shell	−	3.92	0.739	−

[a] R is the Li−Li distance in the core. ρ is the distance from the H_2 c.m. to the closest vertex of the core. r is the H−H distance in the H_2. D is the distance between the first neighbors attached to the same vertex. Complete data on geometry and vibrational frequencies for each cluster are available on request.

TABLE 3: Total Energy of the $Li_3^+(H_2)_n$Clusters Calculated with the 6-311G(2d,2p) Basis Sets (in hartree)[a]

n	i	V_1	V_2	V_3	symm.	E(HF)	E(MP2)	E (MP4)	ΔE
0	0	0	0	0	D_{3h}	−22.173389	−22.193395	−22.201847	−
	1	0	0	0	$D_{\infty h}$	−22.132090	−22.157936	−22.173264	6273
1	0	1	0	0	C_{2v}	−23.310382	−23.361017	−23.377036	−
2	0	1	1	0	C_{2v}	−24.447097	−24.528366	−24.551951	−
	1	2	0	0	C_{2v}	−24.445122	−24.527151	−24.550833	245
3	0	1	1	1	D_{3h}	−25.583508	−25.695427	−25.726574	−
	1	2	1	0	C_S	−25.581565	−25.694268	−25.725522	231
	2	3	0	0	C_S	−25.578977	−25.692987	−25.724362	486
4	0	2	1	1	C_{2v}	−26.717684	−26.861074	−26.899893	−
	1	3	1	0	C_S	−26.715187	−26.859947	−26.898905	217
	2	2	2	0	C_{2v}	−26.715772	−26.859949	−26.898877	223
	3	4	0	0	C_{2v}	−26.710245	−26.856295	−26.895395	987
5	0	3	1	1	C_S	−27.851079	−28.026604	−28.073139	- -
	1	2	2	1	C_{2v}	−27.851584	−28.026480	−28.072972	37
	2	3	2	0	C_S	−27.849235	−28.025558	−28.072202	206
	3	4	1	0	C_S	−27.846360	−28.023150	−28.069832	726
6	0	3	2	1	C_S	−28.984774	−29.191891	−29.246109	- -
	1	2	2	2	D_{3h}	−28.985204	−29.191636	−29.245797	69
	2	3	3	0	C_{2v}	−28.982565	−29.191104	−29.245467	141
	3	4	1	1	C_{2v}	−28.982166	−29.189666	−29.243919	480
	4	4	2	0	C_S	−28.980283	−29.188620	−29.242983	686

[a] For each isomer i, the occupation number V_k indicates the number of H_2 molecules attached to the k vertex of the Li_3^+. ΔE is the energy (in cm^{-1}) of an isomer relative to that of the most stable conformation of the cluster, for a given value of n.

TABLE 4: Müilliken Charges ($\times 10^{-2}$) for the $Li_3^+(H_2)_n$ Clusters[a]

n		$i = 0$	$i = 1$	$i = 2$	$i = 3$	$i = 4$
1	core	19 36 36	–	–	–	–
	q_1	8	–	–	–	–
2	core	22 22 39	16 33 33	–	–	–
	q_1	8	9 9	–	–	–
	q_2	8	–	–	–	–
3	core	25 25 25	18 20 36	11 32 29	–	–
	q_1	8	9 9	9 10 10	–	–
	q_2	8	8	–	–	–
	q_3	8	–	–	–	–
4	core	21 23 23	13 20 32	16 16 33	19 25 25	–
	q_1	8 8	9 9 8	8 8	6 6 9 9	–
	q_2	8	8	8 8	–	–
	q_3	8	–	–	–	–
5	core	15 24 20	19 19 21	11 13 33	21 14 28	–
	q_1	9 9 8	8 8	8 8 9	6 6 8 8	–
	q_2	8	8 8	8 8	8	–
	q_3	8	8	–	–	–
6	core	14 15 22	18 18 18	9 9 30	23 17 17	20 10 26
	q_1	8 8 9	8 8	9 9 8	9 9 5 5	8 8 5 5
	q_2	8 8	8 8	9 9 8	8	8 8
	q_3	8	8 8	–	8	–

[a] For each isomer (n, i), named as in Table 3, the value labeled as "core" gives the charge at each lithium atom, from the more occupied vertex to the less occupied one. With the same convention, q_k is the charge at each H_2 ligand at k vertex.

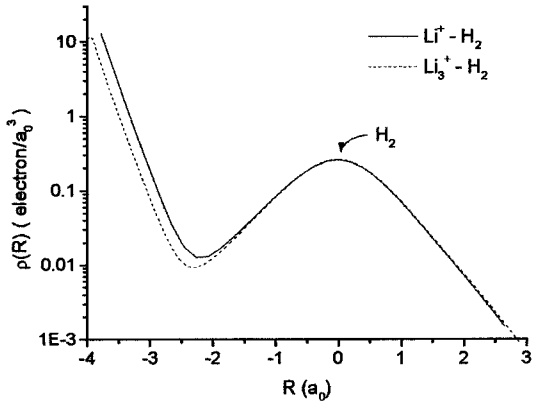

Figure 3. Total electronic density for the $Li^+(H_2)$ and $Li_3^+(H_2)$ clusters along the line connecting the H_2 unit to the lithium atom (in electron/a_0^3), calculated at MP2/6-311G(d,p) level. The right peaks represents the H_2 density. In the case of Li_3^+ core, just the closest lithium atom is shown.

coupled cluster level was 36 cm^{-1}, which is in excellent agreement with the MP4 result.

The distance ρ from each H_2 unit to the vertex of the Li_3^+ core is the same one found for the H_2-core distance in the Li^+-$(H_2)_n$ clusters.[2] Figure 3 shows that the electronic densities along the line connecting the H_2 center-of-mass to the closest lithium atom are approximately the same in both cases. As an H_2 molecule approaches one of the vertex, it gets polarized by the $Li^{\delta+}$ atom on that vertex. As a result of this monopole/induced-dipole interaction, that $Li^{\delta+}$ atom is pulled out from its original position toward the approaching H_2 unit. Thus, the H_2 molecule will experience a field very similar to that of a free Li^+ unit. Alternatively, the similarity between the H_2−core distances can be understood from the structure of the localized molecular orbitals (LMO's)[23] of the Li_3^+ ion. The first three inner LMO's are essentially s-type orbitals centered on each lithium atom. The highest occupied molecular orbital (HOMO) is delocalized through the whole molecule, being responsible for the binding of the triatomic molecule (Figure 4). When a H_2 unit is placed close to its equilibrium position in the cluster, it interacts mainly

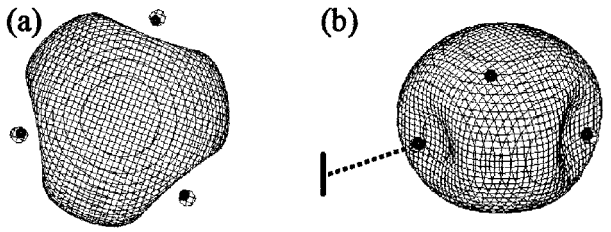

Figure 4. Probability density for the highest occupied localized molecular orbital for the (a) $Li_3^+$and for the (b) $Li_3^+(H_2)$, both calculated at MP2/6-311G(d,p) level.

with the Li atom on the closest vertex. Under this situation, the H_2 unit will experience a field very similar to the one from a free Li^+ slightly screened by the HOMO electrons.

After the monopole/induced-dipole interaction, the main contribution to the core−H_2 bond is the charge transfer from the σ MO of the H_2 molecule to the lowest unoccupied molecular orbital of the positive core. In the case of the H_3^+ core, this transfer is to the 1e′ MO's and reinforces significantly the bond of the H_2 molecules in the first shell.[1] For the Li^+ core, the transfer to 2s atomic orbital is small due to the lower electron affinity of the cation when compared to the $H_2(1\sigma_g)$ ionization potential. For the same reason, the electron transfer to the 2e′ MO's of the Li_3^+ core is also small, and it is even more reduced due to the repulsion from the electrons in the 2a $_1$′ MO.

For the singly occupied vertexes, the configuration in which the H_2 molecular axis stands perpendicular to the Li_3^+ plane is just 0.1 kcal/mol lower than the one with the axis parallel to this plane. The interaction between any two H_2 units occupying different vertexes is negligible, being on the order of 10^{-4} kcal/mol. When bound to the same vertex, the distance (D) between the two first neighbors is about 3 Å, and it is somewhat surprising that for double and triple occupation of a vertex, the most favorable conformation is the one with the H_2 molecular axis almost parallel to each other instead of perpendicular. Different from the $H_3^+(H_2)_n$ core, for which the core vibrational frequencies are approximately equal the frequencies of a free H_3^+ molecule with a solvation effect from the H_2 molecules, the core vibration in the $Li_3^+(H_2)_n$ clusters are mixed with the vibration of the H_2 centers-of-mass (c.m.). This is due to the large difference between the binding energies of the Li_3^+ (−34.7 kcal/mol) and the H_3^+ (−105.9 kcal/mol), which implies that the H_3^+ core preserves its molecular identity more efficiently than the Li_3^+ one. The internal H−H vibrational stretching of the H_2 units are still independent from the motion of their c.m., in agreement with the large binding energy of the H_2 molecule (−107.5 kcal/mol).

3.2. Thermochemical Properties. Assuming that the isomer i of the cluster with n molecules is formed from the most stable isomer ($i = 0$) of the $n - 1$ cluster, its binding energy will be

$$D_e^{(i)}(n) = E(Li_3^+(H_2)_n^{(i)}) - [E(Li_3^+(H_2)_{n-1}^{(0)}) + E(H_2)] \quad (2)$$

The binding energy of the n cluster may be calculated as the thermal average of the binding energy of each one of the isomers, i.e.

$$\langle D_e \rangle_n = \frac{\sum_i D_e^{(i)}(n) \exp[-\Delta E_n^{(i)}/k_B T]}{\sum_i \exp[-\Delta E_n^{(i)}/k_B T]} \quad (3)$$

where k_B and T are the Boltzmann constant and the temperature,

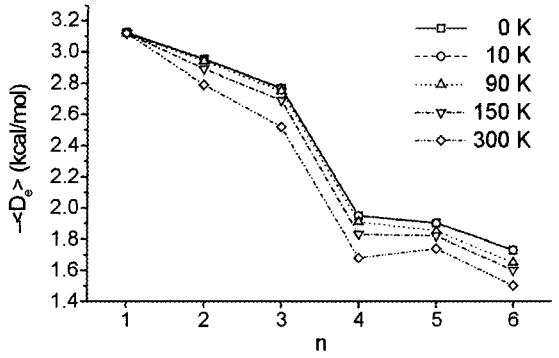

Figure 5. Thermically averaged binding energies $\langle D_e \rangle_n$ of the $Li_3^+(H_2)_n$ clusters calculated with MP2/6-311G(d,p) geometries and with single-point energies obtained at MP4/6-311G(2d,2p) level (in kcal/mol).

TABLE 5: Enthalpy Variation (in kcal/mol) for the $Li_3^+(H_2)_n$ Clusters, Obtained at the MP4/6-311G(2d,2p) Level of Calculation, Using the Vibrational Frequencies and Geometry Optimized at the MP2/6-311G(d,p)

n	$-\Delta H^0_{0K}$	$-\Delta H^0_{50K}$	$-\Delta H^0_{100K}$	$-\Delta H^0_{150K}$	$-\Delta H^0_{200K}$	$-\Delta H^0_{250K}$	$-\Delta H^0_{300K}$
1	1.62	1.96	2.29	2.50	2.54	2.40	2.35
2	1.47	1.82	2.13	2.29	2.29	2.13	2.04
3	1.32	1.67	1.97	2.13	2.11	1.91	1.80
4	0.22	0.57	0.85	1.00	0.96	0.79	0.69
5	−0.05	0.26	0.57	0.76	0.76	0.60	0.53
6	−0.01	0.31	0.58	0.78	0.76	0.59	0.50

respectively. $\Delta E_n^{(i)} = E_n^{(i)} - E_n^{(0)}$ is the energy difference between the ith isomer and the most stable one ($i = 0$) for the a given n.

The binding energy is shown in Figure 5 for several temperatures. For temperatures lower than 100 K, the population of the less stable isomers is very small, and the binding energy is approximately the same as those obtained with just the most stable isomer ($T = 0$ K). As the temperature increases, the thermal effects on the binding energy become more pronounced.

Independently of the temperature, as the cluster increases from $n = 3$ to $n = 4$, one notices an abrupt reduction in the binding energy. This is due to the cluster deformation caused by the double occupation of one of the vertexes, once the fourth H_2 is attached, forcing the other H_2 unit out of the Li_3^+ plane. On the other hand, no abrupt change is observed when the most stable isomer for $n = 5$ (with one of vertexes triply occupied) is formed because only small angular deformations are needed to accommodate the fifth unit.

The enthalpy variation for the clusters formation

$$\Delta H_T^0 = \langle D_e \rangle_n + \epsilon(T) \tag{4}$$

where $\epsilon(T)$ stands for the thermally averaged ZPE + temperature corrections, has been determined at the MP4/6-311G(2d,2p) level of calculation. The zero-point energy (ZPE) corrections were calculated in the harmonic approximation[24,25] with the vibrational frequencies scaled by 0.9223, a factor which results from the comparison between our theoretical frequencies for the $H_3^+(H_2)_n$ and the experimental frequencies from ref 26. The temperature corrections were calculated by assuming ideal behavior for all species and by treating the translational, rotational, and vibrational degrees of freedom classically. Both binding energies and enthalpy variations were corrected for the basis set superposition error (BSSE),[27] which for all clusters is always less than 0.04 kcal/mol.

Results for the variation of the enthalpy are given in Table 5 for several temperatures. Similar to the other hydrogen clusters that we have studied, the formation of the $Li_3^+(H_2)_n$ cluster becomes more exothermic at temperatures from 150 to 200 K. Note that, since we have not calculated the entropy variation for the clustering, it is not possible to verify for what range of temperatures the cluster formation becomes more effective.

3.3. Shell Structure of the Hydrogen Clusters. Several experimental and theoretical works have indicated that the hydrogen molecules are distributed in shells around the positive core. However, there is no consensus on what the shells actually are, how they are formed, and what distinguishes two H_2 molecules belonging to different shells. An attempt to answer these questions has been put forward by Roszak and Leszczynski.[16] On what follows, we will also try to shed some light into this matter by analyzing the several available data on the hydrogen ionic clusters.

We may define a shell in a hydrogen cluster as a set of H_2 molecules presenting similar binding and internal molecular properties. The binding properties can be characterized by the H_2−core distances and the charge transfer from the H_2 units to the core, while the H_2 stretching frequencies and bond distances can be used to define the internal molecular properties.

The main difficulty in identifying H_2 molecules belonging to the same shell resides in the fact that for an incomplete shell the properties mentioned above may not be equal for all H_2 molecules within a shell. For the $H_3^+(H_2)_n$ clusters with incomplete second shell, for example, the H_2−core distance is not a good criterium to distinguish the first from the second shell molecules.[1] In general, the charge transfer, as measured from the Mülliken population, is always a good criterium to distinguish first shell molecules from the second shell ones (see, e.g., ref 13). Identifying a shell may be a complex problem when dealing with cores with asymmetric charge distribution, as is the case of the $CH_3N_2^+$ and the N_2H^+ molecular ions.[17,18] The idea of defining shells simply as concentric distributions of H_2 molecules around the core does not apply in the case of the $CH_3N_2^+(H_2)_n$ clusters, for which three shells are formed in parallels planes, all of them perpendicular to the CN_2 axis.

We distinguish four factors which determine the shell formation and its features:
(1) the coulombian field of the core;
(2) the geometric structure of the core;
(3) the orbital structure of the core;
(4) and the H_2−H_2 interaction.

The relative importance of those effects will depend on the size of the cluster. For instance, the formation of the first shells of ligands will be dominated by the coulombian field of the core. For those shells, one could say that the effects above-mentioned are listed in order of decreasing in importance. However, as the size of the cluster increases, the H_2−H_2 interactions may become the dominant effect in determining the number of ligands in the outer shells, as we will be further discussed.

The core monopole field defines a pattern of radial distribution for the H_2 molecules in all space. This is confirmed by the fact that the neutral $Li(H_2)_n$ clusters do not exhibit radial pattern of ligands, the Li atom remaining at the surface of the cluster.[28]

The geometry of the core determines the symmetry of the ligands distribution. The monatomic cores, X^+, establish a spherically symmetric distribution of H_2 units. For the Li_3^+ case, the positive charge is equally distributed among the Li atoms, and each vertex behaves as a center around which the H_2 units will be spherically distributed. For the N_2H^+ core,[18] the charge is concentrated on the H atom which becomes the center of nucleation, while the N_2 group behaves as a steric barrier to

the approaching H_2 units, thus preventing a spherical distribution of ligands to be formed around the H center.

The nature of the core and of its LUMO (lowest unoccupied molecular orbital) and HOMO orbitals determine the amount of charge transfer from the H_2 molecules to the core. Since a maximum overlap between the core and the H_2 MO's is expected for the ligands closer to the core, the charge transfer process should influence more strongly the structure of the first shell. For the clusters formed by the transition metal cores Co^+, Ni^+, and Cu^+, the first shell contains six, five, and four H_2 molecules, respectively,[13] as a result of the difference in the occupation of the MO's originated from the 3d atomic orbitals.

Finally, the weak interactions among the H_2 molecules should have a more reduced general effect in comparison to the effects due to the coulombian field of the core, which was the reason Roszak and Leszczynski suggested the name shellvation instead of solvation for the shell-distribution phenomena.[16] However, the interaction among the H_2 molecules plays a important role in the structure of the shells by defining, together with the core structure, the maximum number of H_2 molecules in a shell. As for the H_3^+ and the Li_3^+ cores, the three-vertexes structure suggests a pattern of occupation that should be a multiple of three. However, the $H_2-H_3^+$ distance is so small that two H_2 units attached to the same vertex would experience a very repulsive H_2-H_2 interaction. On the other hand, in the case of the Li_3^+ core, the $H_2-Li_3^+$ distance is such that up to four H_2 molecules can be attached to each vertex. For the alkaline atomic ions Li^+ and Na^+, the number of H_2 molecules in the first shell also depends on the H_2-H_2 interactions. The radius of the first shell is determined by the strength of the coulombian field near the core surface, which is larger for the Li^+ core. Consequently, the radius of the first shell will be smaller for the Li^+ core. Therefore, the number of ligands in the first shell of the Li^+ cluster will be smaller than for the Na^+ cluster[2] due to the H_2-H_2 interactions. As the size of the cluster increases, the interaction among the H_2 units may become the dominant effect.

4. Conclusions

According to the present ab initio calculations, $Li_3^+(H_2)_n$ clusters ($n = 1-6$) can be formed as result from the interaction between the Li_3^+ cation and an atmosphere of molecular hydrogen. The structure of these clusters consists of a Li_3^+ triangular core with H_2 molecules attached to the vertexes. The first shell of ligands may contain up to four molecules per vertex, the distance between two closer units on the same vertex being approximately 2.0 Å. For $2 \leq n \leq 6$, several isomers are possible, depending on how the n ligands are distributed among the three vertexes.

The nature of the MO's of the Li_3^+ core is such that each vertex resembles a screened Li^+ ions to which the H_2 units are bound by monopole/induced-dipole interactions. The charge transfer from the H_2 units to the core is much smaller than that in the case of the $H_3^+(H_2)_n$ clusters.

The binding energies are very similar to those obtained for the $Li^+(H_2)_n$ clusters, and they vary from 3 to 1.5 kcal/mol, depending on the size of the cluster. The reaction of formation of the cluster is more exothermic at temperatures between 150 and 200 K.

Acknowledgment. The authors would like to thank Carla Fonseca-Barbatti for reading the manuscript, and the support given by the Brazilian agencies CNPq, FAPERJ, and FINEP.

References and Notes

(1) Barbatti, M.; Ginette Jalbert, Nascimento, M. A. C. *J. Chem. Phys*. **2000**, *113*, 4230.
(2) Barbatti, M.; Ginette Jalbert, Nascimento, M. A. C. *J. Chem. Phys*. **2001**, *114*, 2213.
(3) Barbatti, M.; Ginette Jalbert, Nascimento, M. A. C. *J. Chem. Phys*. **2001**, *114*, 7066.
(4) Louc, S.; Farizon, B.; Farizon, M.; Gaillard, M. J.; Gonçalves, N.; Luna, H.; Jalbert, G.; de Castro Faria, N. V.; Bacchus-Montabonel, M. C.; Buchet, J. P.; Carré, M. *Phys. Rev. A* **1998**, *58*, 3802.
(5) Gobet, F.; Farizon, B.; Farizon, M.; Gaillard, M. J.; Louc, S.; Gonçalves, N.; Barbatti, M.; Luna, H.; Ginette Jalbert, de Castro Faria, N. V.; Bacchus-Montabonel, M. C.; Buchet, J. P.; Carré, M.; Märk, T. D. *Phys. Rev. Lett.* **2001**, *86*, 4263.
(6) Tachikawa, H. *Phys. Chem. Chem. Phys*. **2000**, *2*, 4702.
(7) Chan, M.-C.; Okumura, M.; Oka, T. *J. Phys. Chem. A* **2000**, *104*, 3775.
(8) Ignacio, E. W.; Yamabe, S. *Chem. Phys. Lett*. **1998**, *287*, 563.
(9) Davy, R.; Skoumbourdis, E.; Kompanchenko, T. *Mol. Phys*. **1999**, *97*, 1263.
(10) Curtiss, L. A.; Pople, J. *J. Phys. Chem*. **1988**, *92*, 894.
(11) Bausclicher, C. W., Jr.; Partridge,H.; Langhoff, S. R. *J. Phys. Chem*. **1992**, *96*, 2475.
(12) Kemper, P. R.; Bushnell, J.; Bowers, M. T.; Gellene, G. I. *J. Phys. Chem. A* **1998**, *102*, 8590.
(13) Kemper, P. R.; Weis, P.; Bowers, M. T.; Maıtre, P. *J. Am. Chem. Soc*. **1998**, *120*, 13494.
(14) Weis, P.; Kemper, P.; Bowers, M. T. *J. Phys. Chem. A* **1997**, *101*, 2809.
(15) Doo, D. W.; Lee, Y. T. *J. Chem. Phys*. **1995**, *103*, 520.
(16) Roszak, S.; Leszczynski, J. *Chem. Phys. Lett*. **2000**, *323*, 278.
(17) Gora, R. W.; Roszak, S.; Leszcynski, J. *J. Phys. Chem. A* **1999**, *103*, 9138.
(18) Hiraoka, K.; Katsuragawa, J.; Minamitsu, A.; Ignacio, E. W.; Yamabe, S. *J. Phys. Chem. A* **1998**, *102*, 1214.
(19) Krishnan, R.; Binkley, J. S.; Seeger, R.; Pople, J. A. *J. Chem. Phys*. **1980**, *72*, 650.
(20) Granovsky, A. A. *PC GAMMES*, version 6.0 (http://classic.chem.msu.su/gran/gamess/index.html, accessed Sept 2000).
(21) Schmidt, M. W.; Baldridge, K. K.; Boatz, J. A.; Elbert, S. T.; Gordon, M. S.; Jensen, J. J.; Koseki, S.; Matsunaga, N.; Nguyen, K. A.; Su, S.; Windus, T. L.; Dupuis, M.; Montgomery, J. A. *J. Comput. Chem*. **1993**, *14*, 1347.
(22) Frisch, M. J.; Trucks, G. W.; Schlegel, H. B.; Gill, P. M. W.; Johnson, B. G.; Robb, M. A.; Cheeseman, J. R.; Keith, T. A.; Petersson, G. A.; Montgomery, J. A.; Raghavachari, K.; Al-Laham, M. A.; Zakrzewski, V. G.; Ortiz, J. V.; Foresman, J. B.; Peng, C. Y.; Ayala, P. Y.; Wong, M. W.; Andres, J. L.; Replogle, E. S.; Gomperts, R.; Martin, R. L.; Fox, D. J.; Binkley, J. S.; Defrees, D. J.; Baker, J.; Stewart, J. P.; Head-Gordon, M.; Gonzalez, C.; Pople, J. A. *Gaussian 94*, Revision E.2; Gaussian, Inc.: Pittsburgh, PA, 1995.
(23) Edmiston, C.; Ruedenberg, K. *Rev. Mod. Phys*. **1963**, *35*, 457.
(24) Herzberg, G. *Molecular Spectra and Molecular Structure*; Van Nostrand Reinhold: New York, 1950; Vol. I.
(25) McQuarrie, D. A.; Simon, J. D. *Physical Chemistry - A Molecular Approach*; University Science Books: Sausalito, CA, 1997.
(26) Okumura, M.; Yeh, L. I.; Lee, Y. T. *J. Chem. Phys*. **1988**, *88*, 79.
(27) Chen, W.; Gordon, M. S. *J. Phys. Chem*. **1996**, *100*, 14316.
(28) Scharf, D.; Martyna, G. J.; Klein, M. L. *J. Chem. Phys*. **1993**, *99*, 8997. Scharf, D.; Martyna, G. J.; Li, D.; Voth, G. A.; Klein, M. L. *J. Chem. Phys*. **1993**, *99*, 9013.